Crystal Structure and Magnetic Ordering of Manganites $La_{0.7}Ca_{0.3}Mn_{1-y}Fe_yO_3$

Abstract—The influence of the replacement of Mn ions in the $La_{0.7}Ca_{0.3}Mn_{1-y}Fe_yO_3$ compounds ($0 \leq y \leq 0.09$) by another transitional metal, Fe, was studied. The radii of both ions are almost identical, which makes the effect of the transitional metal on the physical properties of manganites more transparent. The crystal structure of three samples (with $y = 0, 0.03, 0.09$) is studied in the temperature range $T = 1.5$–300 K by neutron powder diffraction. All investigated samples belong to the orthorhombic space group $Pnma$ (62). It is confirmed that Fe ions occupy the Mn positions in the unit cell. As the Fe concentration increases, the saturation value of the spontaneous magnetic moment and the Curie temperature decrease, but the ground state remains ferromagnetic for $0 \leq y \leq 0.1$. The saturation values of the magnetic moments at $T = 1.5$ K are $m_{FM} = 3.72(3)$, $3.40(3)$, and $3.27(3)$ μ_B/Mn for the samples with an Fe concentration $y = 0, 0.03$, and 0.09, respectively.

1. INTRODUCTION

A drastic change in the resistivity $\rho(T)$ accompanied by a paramagnetic–ferromagnetic (FM) transition in perovskite manganites was one of the main reasons for the revived interest in these compounds [1, 2], which were first studied as early as in the 1950s [3, 4]. In recent years, colossal magnetoresistance (CMR), different kinds of magnetic ordering [2, 5–7], the metal–insulator transition [1–5], charge ordering [8–10], and phase separation [11] have been intensively studied in manganites and related compounds. The properties of perovskite manganites are determined by the double exchange in the Mn^{3+}–O–Mn^{4+} complex and the Jahn–Teller effect due to the Mn^{3+} ions [3, 4, 12].

Partial substitution of divalent ions (A = Ca, Sr, Ba, Pb) for La^{3+} in hole-doped $La_{1-x}A_xMnO_3$ manganites leads to a deviation of the Mn–O–Mn bond angle from 180° and changes the Mn–O bond length in the perovskite lattice. Simultaneously, the interaction between Mn^{3+} and Mn^{4+} changes, which affect the FM ordering mechanism (double exchange) [13]. The main building block determining the properties of the manganites ABO_3 is the MnO_6 octahedron. Substitution of a small amount of ions at the B sites by other transitional metals, such as Fe^{3+} [14–28], which has an ionic radius close to that of Mn^{3+} [29], affects the charge ordering and the double exchange interaction [15, 19]. Although the properties of the $La_{1-x}Ca_xMn_{1-y}Fe_yO_3$ (LCMFO)

compounds, such as the temperature and field dependences of the resistivity, the magnetothermoelectric power, and magnetization [14–25], have been studied quite thoroughly in the hole doping range $x < 0.5$, the structure and especially the features of the magnetic phase diagram of the $La_{1-x}Ca_xMn_{1-y}Fe_yO_3$ compounds are not so well known.

We are aware of just two publications devoted to investigation of the LCMFO structure at low temperatures using neutron powder diffraction [26, 27]. The results obtained in those studies are very different. In [26], a sample of $La_{0.67}Ca_{0.33}Mn_{0.9}Fe_{0.1}O_3$ was studied over the temperature range 15–150 K. The neutron diffraction patterns in the low-angle range 12°–33°, where the magnetic scattering intensity is expected to be maximum, are absolutely identical at all temperatures and correspond well to an only crystallographic phase; i.e., no long-range magnetic ordering is observed. In [27], three samples of the $La_{0.66}Ca_{0.34}MnO_3$, $La_{0.66}Ca_{0.34}Mn_{0.9}Fe_{0.1}O_3$, and $La_{0.66}Ca_{0.34}Mn_{0.8}Fe_{0.2}O_3$ compositions were studied over the temperature range 15–150 K. For all three compositions, a noticeable magnetic contribution is observed in neutron diffraction pattern at low temperatures and the magnetic ordering is purely FM. In order to resolve the discrepancies between the data on the magnetic properties of $La_{1-x}Ca_xMn_{1-y}Fe_yO_3$ reported in [26] and [27], we performed high-resolution neutron powder diffraction measurements over a wide temperature range.

Structural parameters (lattice parameters and interatomic distances and bond angles in the MnO_6 octahedron) derived from the experimental neutron diffraction patterns for $La_{0.7}Ca_{0.3}MnO_3$, $La_{0.7}Ca_{0.3}Mn_{0.97}Fe_{0.03}O_3$, and $La_{0.7}Ca_{0.3}Mn_{0.91}Fe_{0.09}O_3$

	$La_{0.7}Ca_{0.3}MnO_3$		$La_{0.7}Ca_{0.3}Mn_{0.97}Fe_{0.03}O_3$		$La_{0.7}Ca_{0.3}Mn_{0.91}Fe_{0.09}O_3$	
	$T = 1.5$ K	$T = 300$ K	$T = 1.5$ K	$T = 300$ K	$T = 1.5$ K	$T = 300$ K
Lattice parameters, Å						
a	5.4550(1)	5.4655(1)	5.4664(2)	5.4674(2)	5.4596(1)	5.4685(1)
$b/\sqrt{2}$	5.4499(1)	5.4612(1)	5.4513(3)	5.4634(3)	5.4536(2)	5.4642(2)
c	5.4679(1)	5.4812(1)	5.4681(3)	5.4794(3)	5.4730(2)	5.4813(2)
V_0, Å^3	229.89(1)	231.37(1)	230.02(3)	231.47(3)	230.45(2)	231.63(2)
Interatomic distances, Å						
$Mn–O1 \times 2$	1.9544(9)	1.9632(6)	1.954(1)	1.9706(9)	1.960(1)	1.965(1)
$Mn–O21$	1.951(3)	1.959(2)	1.948(5)	1.948(5)	1.958(4)	1.961(4)
$Mn–O22$	1.968(3)	1.966(2)	1.973(5)	1.973(4)	1.967(4)	1.962(4)
Interatomic bond angles, deg						
$Mn–O1–Mn$	160.7(1)	159.2(1)	161.0(1)	156.6(1)	159.8(1)	156.9(1)
$Mn–O2–Mn$	160.5(1)	160.9(1)	160.1(2)	160.0(2)	159.7(2)	161.4(2)

2. EXPERIMENT

$La_{1-x}Ca_xMn_{1-y}Fe_yO_3$ samples ($x = 0.3$; $y = 0$, 0.03, 0.09) were prepared using a standard solid-state ceramic method. Stoichiometric mixtures of La_2O_3, $CaCO_3$, MnO_2, and Fe_2O_3 were annealed in air at 1320°C for 15 h, then for 5 h, and again for 15 h. The samples were ground between annealings. The powders thus obtained were pressed into pellets using a pressure of 2000 kg/cm^2. The pellets were annealed at 1375°C for 22 h and then were powdered again.

Neutron diffraction measurements were performed using a G4.2 Russian–French high-resolution neutron powder diffractometer, which was installed on a cold-neutron guide of the ORPHEE reactor in the Leon Brillouin Laboratory (Saclay, France) and has 70 detectors in seven sections [30]. Neutron diffraction patterns were recorded in the superposition mode using monochromatic neutrons ($\lambda = 2.3428$ Å) over the angular range $3° \le 2\theta \le 174°$. For the measurements, powder samples were placed in a vanadium container 8 mm in diameter. Samples were cooled to 1.5 K in liquid helium. Diffraction patterns were recorded during heating at $T = 1.5$, 200, 250, 260, and 300 K for the $La_{0.7}Ca_{0.03}MnO_3$ compound; at $T = 1.5$, 150, 210, 230, and 300 K for the $La_{0.7}Ca_{0.3}Mn_{0.97}Fe_{0.03}O_3$ compound; and at $T = 1.5$, 100, 130, 135, 150, and 300 K for the $La_{0.7}Ca_{0.3}Mn_{0.91}Fe_{0.09}O_3$ compound. These modes of operation were chosen based on the temperature dependences of the magnetic susceptibility $\chi_{dc}(T)$, which were measured for the samples beforehand [21]. We chose the lowest available temperature (1.5 K) at which full magnetic ordering was certainly achieved (Fig. 1); room temperature (≈ 300 K), at which all compounds are paramagnetic; and also several temperatures around (both above and below) the onset of magnetic ordering.

3. CRYSTAL STRUCTURE

Figure 1 shows several experimental neutron diffraction patterns measured for $La_{0.7}Ca_{0.3}Mn_{1-y}Fe_yO_3$ samples at $T = 1.5$ K (in the magnetic-ordering region) and at temperatures above the Curie temperature T_C, where the compounds under study are paramagnetic ($T = 260$, 230, and 150 K for samples with a Fe content $y = 0$, 0.03, and 0.09, respectively). The crystal structures and their parameters were refined using the Rietveld method with the FULLPROF software [31]. The crystal structures of all three samples in the tem-
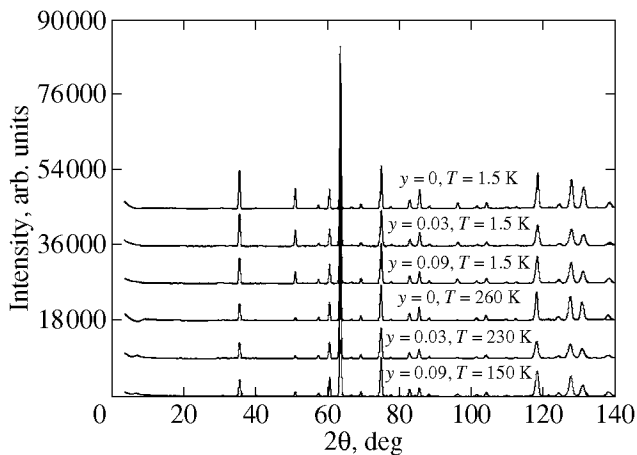

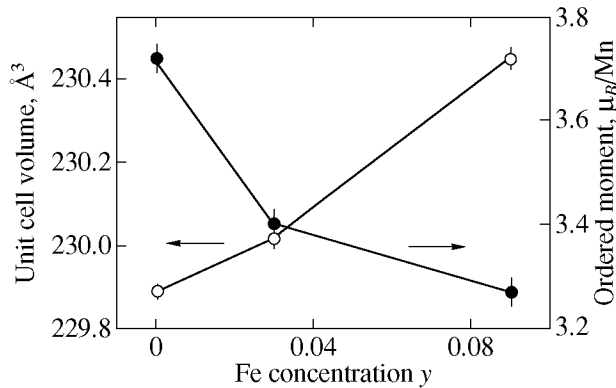Fig. 1. Experimental neutron diffraction patterns recorded at $T = 1.5$ K (in the magnetic ordering region) and at temperatures slightly above T_C ($T = 260$, 230, and 150 K for $La_{0.7}Ca_{0.3}Mn_{1-y}Fe_yO_3$ with an Fe content $y = 0$, 0.03, and 0.09, respectively).

Fig. 2. Unit cell volume and the saturation value of the Mn magnetic moment as functions of the Fe concentration in $La_{0.7}Ca_{0.3}Mn_{1-y}Fe_yO_3$ samples.

Fig. 3. Example of the refinement of the neutron diffraction pattern of $La_{0.7}Ca_{0.3}Mn_{0.91}Fe_{0.09}O_3$ measured at $T = 1.5$ K. Open circles are experimental data, and the solid line is the result of processing the diffraction pattern using the Rietveld method. The difference curve (between the experimental data and the calculation) is shown by the solid line in the lower part of the figure. The Bragg reflections for the nuclear and ferromagnetic structures are shown by vertical bars.

perature range 1.5–300 K are described well by the orthorhombic space group *Pnma* (62) typical of manganites. It is established unambiguously that Fe ions substitute for Mn ions at their positions in the unit cell. This fact directly confirms the conjecture stated in several papers [15, 17, 32] that iron ions substitute for manganese and corrects earlier publications wherein it was reported that LCMFO samples have an undistorted cubic unit cell with space group *Pm3m* [21–23]. The reason for this error was in the use of x-ray powder diffraction. The low sensitivity of the equipment employed prevented detection of small lattice distortions of the order of 0.15%.

The table gives the main structural parameters (the lattice constants and the interatomic distances and bond angles in the MnO_6 octahedron) obtained using high-resolution neutron powder diffraction at $T = 1.5$ and 300 K. The values of the lattice constants indicate that the unit cell satisfies the condition $b/\sqrt{2} < a < c$ at all temperatures. At both $T = 1.5$ and 300 K, the lattice constants and, accordingly, the unit cell volume increase almost linearly with the Fe content (Fig. 2). These results are in good agreement with the increase in all three lattice constants in $La_{0.7}Ca_{0.3}Mn_{1-y}Fe_yO_3$ [17] and $La_{0.5}Ca_{0.5}Mn_{1-y}Fe_yO_3$ [19] established in experiments on x-ray powder diffraction. The linear increase in the lattice constants and the unit cell volume with the Fe content is unexpected, because the ionic radius of Fe^{3+} is almost equal to that of Mn^{3+}. The valence of Fe atoms (3+) in these compounds was established earlier in Mössbauer experiments [18, 28]. However, the absolute opposite result was obtained in [27] by neutron powder diffraction for $La_{0.66}Ca_{0.34}MnO_3$, $La_{0.66}Ca_{0.34}Mn_{0.9}Fe_{0.1}O_3$, and $La_{0.66}Ca_{0.34}Mn_{0.8}Fe_{0.2}O_3$ samples, where the lattice constants were found to decrease with increasing Fe content.

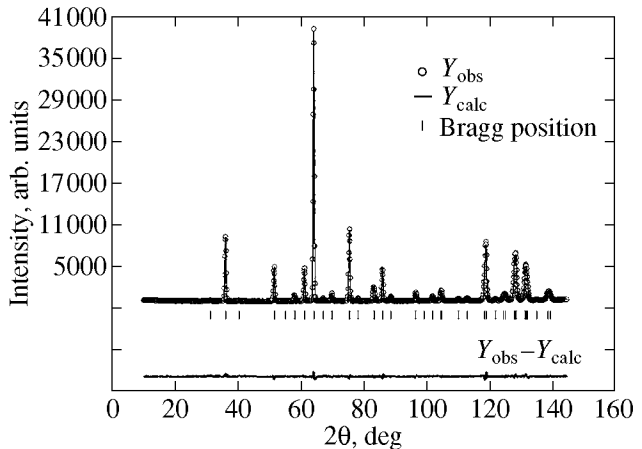The distances between the ions in the MnO_6 octahedron (Mn–O1, Mn–O2, Mn–O22) differ only slightly

and are, on the average, 1.962 Å. The value for the apical Mn–O1 bond length lies between the equatorial bond lengths. The Mn–O–Mn bond angles turned out to be significantly different from 180° and are roughly equal for all three compositions, despite significant differences between the magnetic ordering temperatures. The Mn–O1–Mn and Mn–O2–Mn bond angles differ at room temperature and are $\approx 157°$ and 161°, respectively. These angles become almost equal ($\approx 160°$) at $T = 1.5$ K.

4. MAGNETIC STRUCTURE

The magnetic contribution is clearly seen in the neutron diffraction patterns at $T = 1.5$ K (Fig. 1). The variations in the first strong reflection (at $2\theta \approx 35.1°$) indicate that this contribution decreases with an increase in the Fe content.

The magnetic contribution to the neutron diffraction patterns at low temperatures is also analyzed using the Rietveld method with the FULLPROF software. We used only a single-phase homogeneous model for the Mn sublattice and assumed that the crystals have an orthorhombic *Pnma* lattice.

The analysis unambiguously indicates that the magnetic ground state of all compounds under study is homogenous and purely FM. The closeness of the fitting to the experimental data can be seen in Fig. 3, which shows the result of analyzing the experimental neutron diffraction pattern of $La_{0.7}Ca_{0.3}Mn_{0.91}Fe_{0.09}O_3$ measured at $T = 1.5$ K.

The saturation values of the magnetic moments m_{FM} at $T = 1.5$ K are 3.72(3), 3.40(3), and 3.27(3) μ_B/Mn for $y = 0$, 0.03, and 0.09, respectively (Fig. 2). Because the
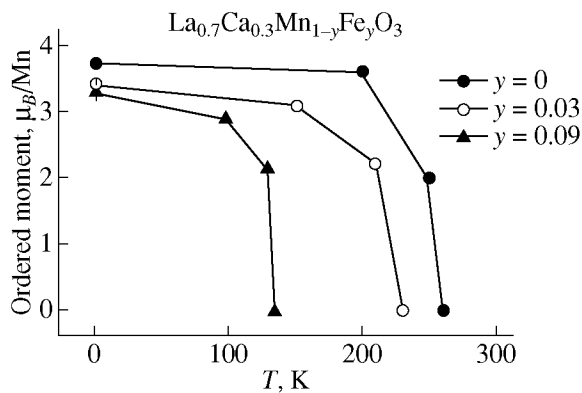
Fig. 4. Temperature dependences of the Mn magnetic moments for three $La_{0.7}Ca_{0.3}Mn_{1-y}Fe_yO_3$ samples ($y = 0$, 0.03, 0.09) derived from the experimental neutron diffraction patterns.

differences between the lattice parameters are small, the diffractometer resolution does not allow unique determination of the direction of the FM moments. Figure 4 shows the temperature dependences of the magnitude of the FM moments for all three compounds under study.

5. DISCUSSION

In [26, 27], the magnetic properties of $La_{1-x}Ca_xMn_{1-y}Fe_yO_3$ compounds were studied over temperature and composition ranges comparable to those covered in the present paper. According to the Mössbauer spectroscopy data [27], the Fe ions substituting for Mn ions are in the Fe^{3+} state ($S = 5/2$) and the interaction between the Fe and Mn ions in the perovskite lattice is antiferromagnetic. Investigations of the magnetic susceptibility of ceramic $La_{1-x}Ca_xMn_{1-y}Fe_yO_3$ samples in weak dc magnetic fields ($B = 2$–80 Oe) showed that T_C decreases from 259 to 107 K as the Fe concentration increases in the range $0 \le y \le 0.09$. The LCMFO compounds undergo a transition from the weakly frustrated FM phase with an Fe content $y \cong 0$–0.05 to a strongly frustrated phase (with $y \cong 0.07$–0.10), which is confirmed by observations of magnetic irreproducibility and long relaxation times (up to $t = 10^5$ s) of the residual magnetization [21, 22]. The strongly frustrated state is a mixture of the FM phase and a spin-glass phase. When Fe is introduced into a sample, the magnetization and T_C decrease and the resistivity increases. In [1, 15, 25], it was shown that the resistivity maximum corresponding to the metal–insulator transition was shifted to lower temperatures with an increase in the Fe content. Iron doping affects the Mn^{3+}/Mn^{4+} ratio and the number of sites suitable for hopping. Electrons can hop between Mn^{3+} and Mn^{4+} but cannot hop between Mn^{3+} and Fe^{3+} sites. So, even a small amount of Fe ($y = 0.01$–0.1) has a strongly effect on the transport and magnetic properties of LCMFO [21, 22, 25].

Iron atoms form Fe^{3+}–Mn^{4+} pairs and introduce an antiferromagnetic superexchange interaction, thereby suppressing the double exchange mechanism. This fact is clearly illustrated by Fig. 4, where the temperature dependences of the magnetic moments are shown for samples with different Fe contents.

6. CONCLUSIONS

Our neutron diffraction measurements, as well as previous studies of compounds with $y = 0$ [33, 34], have demonstrated that, below the magnetic phase transition point T_C, manganites $La_{0.7}Ca_{0.3}Mn_{1-y}Fe_yO_3$ are in a homogeneous ferromagnetic state. It has also been established that, as the Fe concentration increases, the saturation value of the spontaneous magnetic moment and the Curie temperature decrease. It has been shown that Fe doping to levels in the range $0 \le y \le 0.1$ does not change the nature of magnetic ordering in LCMFO. Therefore, our results on magnetic ordering completely confirm the data from [27] obtained for slightly different Fe contents: $y = 0.1$ and 0.2.

REFERENCES

1. P. Schiffer, A. P. Ramirez, W. Bao, and S.-W. Cheong, Phys. Rev. Lett. **75**, 3336 (1995).
2. K. Chahara, T. Ohno, M. Kasai, and Y. Kozono, Appl. Phys. Lett. **63**, 1990 (1993).
3. C. Zener, Phys. Rev. **82**, 403 (1951).
4. J. B. Goodenough, Phys. Rev. **100**, 564 (1955).
5. A. P. Ramirez, J. Phys.: Condens. Matter **9**, 8171 (1997).
6. R. Laiho, E. Lähderanta, J. Salminen, K. G. Lisunov, and V. S. Zakhvalinskii, Phys. Rev. B: Condens. Matter **63**, 094405 (2001).
7. R. Laiho, K. G. Lisunov, E. Lähderanta, P. Petrenko, J. Salminen, V. N. Stamov, and V. S. Zakhvalinskii, J. Phys.: Condens. Matter **12**, 5751 (2000).
8. C. H. Chen and S.-W. Cheong, Phys. Rev. Lett. **76**, 4042 (1996).
9. M. Roy, J. F. Mitchell, A. P. Ramirez, and P. Schiffer, J. Phys.: Condens. Matter **11**, 4843 (1999).
10. Y. Moritomo, Phys. Rev. B: Condens. Matter **60**, 10374 (1999).
11. M. Hennion, F. Moussa, G. Biotteau, J. Rodriguez-Carvajal, L. Pinsard, and A. Revcollevschi, Phys. Rev. Lett. **81**, 1957 (1998).
12. A. J. Millis, P. B. Littlewood, and B. I. Shraiman, Phys. Rev. Lett. **74**, 5144 (1995).
13. H. Y. Hwang, S.-W. Cheong, P. G. Radaelli, M. Marezio, and B. Batlogg, Phys. Rev. Lett. **75**, 914 (1995).
14. L. Righi, P. Gorria, M. Insausti, J. Gutiérrez, and J. M. Barandiarán, J. Appl. Phys. **81**, 5767 (1997).

15. K. H. Ahn, X. W. Wu, K. Liu, and C. L. Chien, Phys. Rev. B: Condens. Matter **54**, 15299 (1996).

16. J. W. Cai, C. Wang, B. G. Shen, J. G. Zhao, and W. S. Zhan, Appl. Phys. Lett. **71**, 1727 (1997).

17. J. R. Sun, G. H. Rao, B. J. Shen, and H. K. Wong, Appl. Phys. Lett. **73**, 2998 (1998).

18. S. B. Ogale, R. Sheekala, R. Bathe, S. K. Date, S. I. Patil, B. Hannooyer, F. Petit, and G. Marest, Phys. Rev. B: Condens. Matter **57**, 7841 (1998).

19. X. Chen, Z. Wang, R. Li, B. Shen, W. Zhan, J. Sun, J. Chen, and Ch. Yan, J. Appl. Phys. **87**, 5594 (2000).

20. H. Song, W. Kim, S. J. Kwon, and J. Kang, Appl. Phys. **89**, 3398 (2001).

21. R. Laiho, K. G. Lisunov, E. Lähderanta, J. Salminen, V. N. Stamov, and V. S. Zakhvalinskii, J. Magn. Magn. Matter **250**, 267 (2002).

22. R. Laiho, K. G. Lisunov, E. Lähderanta, J. Salminen, M. A. Shakhov, V. N. Stamov, P. A. Petrenko, and V. S. Zakhvalinskii, J. Phys. Chem. Solids **64**, 1573 (2003).

23. R. Laiho, K. G. Lisunov, E. Lähderanta, P. A. Petrenko, J. Salminen, M. A. Shakhov, M. O. Safontchik, V. N. Stamov, M. L. Shubnikov, and V. S. Zakhvalinskii, J. Phys.: Condens. Matter **14**, 8043 (2002).

24. R. Laiho, K. G. Lisunov, E. Lähderanta, V. N. Stamov, V. S. Zakhvalinskii, A. I. Kurbakov, and A. E. Sokolov, J. Phys.: Condens. Matter **16**, 881 (2004).

25. R. Laiho, E. Lähderanta, J. Salminen, K. G. Lisunov, V. S. Zakhvalinskii, M. O. Safontchik, M. A. Shakhov, and M. L. Shubnikov, J. Appl. Phys. **91**, 7400 (2002).

26. S. M. Yusuf, M. Sahana, M. S. Hegde, K. Dörr, and K. H. Müller, Phys. Rev. B: Condens. Matter **62**, 1118 (2000).

27. A. Simopoulus, M. Pissas, G. Kallias, E. Devlin, N. Moutis, I. Panagiotopoulos, D. Niarchos, C. Christides, and R. Sonntag, Phys. Rev. B: Condens. Matter **59**, 1263 (1999).

28. M. Pissas, G. Kallias, E. Devlin, A. Simopoulus, and D. Niarchos, J. Appl. Phys. **81**, 5770 (1997).

29. R. D. Shannon, Acta Crystallogr., Sect. A: Cryst. Phys., Diffr., Theor. Gen. Crystallogr. **32**, 751 (1976).

30. A. I. Kurbakov, V. A. Trounov, T. K. Baranova, A. P. Bulkin, R. P. Dmitriev, Ya. A. Kasman, J. Rodriguez-Carvajal, and T. Roisnel, Mater. Sci. Forum **321–324**, 308 (2000).

31. J. Rodriguez-Carajal, Physica B (Amsterdam) **192**, 55 (1993).

32. G. H. Jonker, Physica (Amsterdam) **20**, 1118 (1954).

33. P. G. Radaelli, D. E. Cox, M. Marezio, S.-W. Cheong, P. E. Schiffer, and A. P. Ramirez. Phys. Rev. Lett. **75**, 4488 (1995).

34. Q. Huang, A. Santoro, J. W. Lynn, R. W. Erwin, J. A. Borchers, G. L. Peng, K. Ghosh, and R. L. Greene, Phys. Rev. B: Condens. Matter **58**, 268 (1998).